Proceedings of the OCEANS 2005 MTS/IEEE Conference & Exhibition
Washington, D.C. USA

ISBN CD-ROM: 0-933957-33-5

Additional copies of this publication are available from

Marine Technology Society, 5565 Sterrett Place, Suite 108, Columbia, MD 21044 USA
Tel: +1 410-884-5330, Fax +1 410-884-9060, email: mtsmbrship@erols.com

IEEE Operations Center, P.O. Box 1331, 445 Hoes Lane, Piscataway, NJ 08855-1331 USA
Tel: +1 800 678 IEEE, +1 732 981 1393, Fax: +1 732 981 9667, email: customer.services@ieee.org

Produced by: Veraprise Incorporated, P. O. Box 949 Front Royal, VA 22630
Tel: +1 540-631-0919, Fax: +1 540-631-3464, http://www.veraprise.com/, ebusiness@veraprise.com

Bathymetry of shallow coastal regions derived from space-borne hyperspectral sensor

ZhongPing Lee, Brandon Casey, Rost Parsons, Wesley Goode, Alan Weidemann, and Robert Arnone

Naval Research Laboratory
Code 7333
Stennis Space Center, MS 39529
zplee@nrlssc.navy.mil

Abstract

Hyperion is a hyperspectral sensor on board NASA's EO-1 satellite. Its spatial resolution is about 30 meters with a swath of ~7 Km. Though Hyperion was not designed for ocean studies, its unique spectral configuration (430 nm – 2400 nm with a ~10nm step) makes it especially attractive to study the effectiveness of such kind of sensor for observing complex coastal waters. In this study, Hyperion data over two sites of the Florida coasts were acquired, with one focused on the clear Key West waters, and the other focused on the relatively turbid Tampa Bay waters. From both data sets, water properties and bottom bathymetry were simultaneously derived from atmosphere-corrected Hyperion data using a spectral matching technique. More importantly, in the top-to-bottom processing of Hyperion data, there was no use of any *a prior* or ground truth information. For the Key West site, derived bathymetry and water properties were validated with NAVOCEANO CHARTS (active bathymetric LIDAR system) and field measurements, respectively. It is found that the retrieved depths (in a range of ~ 1 – 20 m) match LIDAR depths very well (~15% average error), indicating significant potential of using hyperspectral satellite sensor for efficient and repetitive observation of shallow coastal regions.

1. Introduction

For many Navy operations, environmental information of coastal waters is critical and impacts the success or failure of the mission. In shallow waters (less than 20 meters) the optical properties, bottom reflectivity, and depth are all essential elements in the performance of mine Electro-optical Identification (EOID) systems. The Navy also uses active electro-optical sensors for high resolution surveys of coastal bathymetry and shoreline characteristics. Systems such as the CHARTS (Compact Hydrographic Airborne Rapid Total Survey) sensors employ both active and passive high resolution sensors in the visible range of the spectrum. However, knowing when and where conditions are favorable for utilization of such assets effects cost and efficiency of all electro-optical sensors.

For shallow coastal waters, Lee and Carder [1] have demonstrated that reliable derivation of water and bottom properties from spectral remote sensing requires a sensor with hyperspectral capability. Current operational satellite sensors designed for observation of water properties, such as SeaWiFS or MODIS, however, have few spectral bands along with a large spatial footprint. Such sensors are unable to provide the detailed and accurate information for shallow coastal environments.

The Hyperion sensor on board the EO-1 platform [2], designed for land observations, however, has wavelength bands from ~430 nm to 2400 nm with a ~10 nm resolution. Also, the ground resolution of the sensor is about 30 meters. Such spectral and spatial characteristics are significantly better suited for the study of coastal waters than the sensors such as SeaWiFS or MODIS. But the limitation of this sensor is its low signal-to-noise ratios compared to SeaWiFS or MODIS.

The low signal-to-noise ratio has big impact on water observation. Water targets typically have much weaker signals than land targets. Hyperion, being designed for land operations, did not require a high signal-to-noise ratio. Hyperion then may not have enough sensitivity to "differentiate" the subtle change of water properties. Consequently it was perceived that Hyperion would have little usefulness for water studies. For many shallow coastal area, however, due to the increased turbidity of water and strong reflectance from the bottom, the signals emanating from the water could be much stronger than that from oceanic waters. Therefore, as indicated in an earlier study by Brando and Dekker [3], Hyperion imagery could be very useful for coastal areas and for Navy operations.

In this study, using Hyperion data collected over the Florida Keys as an example, we present an innovative and practical method for the derivation of remote-sensing reflectance (Rrs) for such an imperfect sensor. Hyperion Rrs is further applied to a newly developed hyperspectral optimization processing scheme (HOPE) for the derivation of water and bottom properties. Unlike traditional empirical regressions that require many assumptions and ground truth data to derive bathymetry from Rrs [4, 5], HOPE is fully automated and free of the requirement for ground information. Hyperion derived water and bottom properties are further compared with in-situ measurements and shown to be in excellent agreement. These results indicate that with the innovative method of deriving Rrs and the advanced optimization algorithm for water properties, Hyperion imagery can provide vital and reliable information at least for shallow coastal environments.

2. Data

L1A Hyperion data over Looe Key (Florida) collected on October 26, 2002 was provided by the USGS. Since our focus is on water and bottom properties, only information from 430 – 925 nm was used. The image was centered at 24°42'39" (N), 81°22'15" (W). Figure 1 presents the collection area and a subset of the image. This subset includes clear oceanic waters, shallow sandy bottom waters, and complex out flows from nearby land with mangroves.

During the collection of Hyperion data, bathymetry of the study area was surveyed with the SHOALS system (an earlier version of CHARTS) – an active bathymetric LIDAR system. In-situ measurements of remote-sensing reflectance and water's optical properties were also collected at six sites in the area (see red dots of Fig.1), with Rrs measured by a custom-made spectroradiometer and water absorption coefficients measured by AC-9 (Wetlabs, Inc.).

3. Methodology to derive remote sensing reflectance

To analytically derive water and/or bottom properties from any satellite data, the first step is to get high quality data of remote-sensing reflectance (Rrs), which is defined as the ratio of water-leaving radiance (L_w) to downwelling irradiance just above the surface (Ed). It is Rrs that solely contains water and/or bottom information.

In general, the radiance measured by a sensor at any altitude (L_t) can be expressed as

$$L\_t = L\_sky + t*L\_w, \qquad (1)$$

with L_sky for contributions from the sky and L_w for contributions from below the water surface. t is the transmittance of L_w from sea surface to sensor altitude. From the definition of Rrs, one obtains

$$Rrs = (L\_t - L\_sky)/(t*Ed). \qquad (2)$$

To obtain R_{rs} from L_t, L_sky, t, and Ed must be known. Traditionally, standard methods calculate L_sky, t, and Ed based on models of radiative transfer in the atmosphere [6, 7]. Since L_w in general makes up about 10% of L_t, such methods require high accuracy in the measured L_t (error of within 1% for ocean applications) and high accuracy of aerosol models. The Hyperion sensor, however, has an accuracy of within 5% in the measured L_t [8]. The L_t error may cause a 50% error in L_w which in turn can cascade into significant uncertainties in derived water properties. For such a poorly calibrated satellite or aircraft sensor, an innovative method is required.

To meet such a goal, we developed a practical and reliable technique to derive Rrs from Hyperion data. This technique is an extension of the cloud-shadow method developed by Reinersman et al. [9]. In that method [9], L_sky is calculated from pair of adjacent pixels that is under cloud shadow and under the Sun, with t and Ed calculated from radiance transfer with models for aerosols. It also required the sensor to be well calibrated radiometrically and spectrally.

In our technique, we calculate L_sky in a similar but simplified fashion of that of Reinersman et al. [9], but t and Ed are evaluated quite differently. In our technique, t and Ed are not explicitly derived. Instead, the product of t and Ed is estimated using the reflected radiance from the top of the cloud. Specifically, for the pixel under the Sun, its radiance (L_t1) is expressed as:

$$L\_t1 = L\_sky1 + t*Ed*Rrs. \qquad (3)$$

For the pixel under the cloud, its radiance (Lt_2) is

$$L\_t2 = L\_sky2 + t*Ed\_sky*Rrs. \qquad (4)$$

Fig.2a shows the locations of a pair of such pixels with the corresponding L_t1 and L_t2 from Hyperion in Fig.2b.

If we assume that L_sky1 = L_sky2 = L_sky, then one can get

$$L\_sky = L\_t1 - (L\_t1 - L\_t2)/(1-Ed\_sky/Ed). \qquad (5)$$

The ratio of Ed_sky/Ed is estimated using Radtran [10], L_sky is then easily calculated from Eq.5, in units that is the same as L_t from the sensor, either in raw counts or units of absolute radiance. Fig.2c presents the calculated L_sky of this study.

To calculate Rrs, values of t*Ed are still needed. For this component, we use the radiance from the cloud top to make the estimation. As above, radiance from a cloud top can be expressed as

Lt_cloud = L_sky + t*Ed*Rrs_cloud. (6)

Fig.2d shows averaged Lt_cloud of a few randomly collected cloud-top radiance. Lastly, Rrs at any pixel can be calculated as

Rrs = (L_t – L_sky)/(Lt_cloud – L_sky)*Rrs_cloud. (7)

Fig.2e presents the calculated Rrs for the pixel under the Sun (Fig.2b), with a spectrally constant Rrs_cloud value of 0.159 (a value derived based on the absolute radiance of L_cloud used in the calculation). This spectral Rrs shows reasonable values and spectral shapes as commonly observed in literature. And, the Rrs shows smooth spectral variation in the 430 – 800 nm range, as compared to the slightly noise Rrs obtained by Brando and Arnold [3], though both were high signal coastal waters.

One obvious advantage of this new approach is that L_t, L_sky, and L_cloud are all measured by the same sensor at the same time; therefore the derived Rrs has no dependence on the accuracy of L_t, because sensor's response function (calibration factor) is canceled out. Also, since L_sky is the smaller spectrum of the image, Rrs calculated by this method will normally be positive in the short wavelengths. This method, however, does depend on the assumption that L_sky is nearly uniform for the small study area.

By applying Eq.7 to the entire Hyperion image, Rrs is calculated for each pixel within the scene. Fig.3 compares the Rrs from Hyperion to Rrs from in-situ measurements using this technique. Excellent agreement between the Hyperion Rrs and the in-situ Rrs is demonstrated in four out of the six in-situ stations (including the offshore clear water station), in both spectral shape and spectral values. However, for two stations (St.2 and St.5), while the spectral shape of the two Rrs are quite consistent, the Hperion Rrs are significantly higher than in-situ Rrs. The reasons for this mismatch are not clear and further analysis is required.

4. Retrieval of environmental properties

To derive properties of the water column and bottom from Rrs, we applied the optimization approach developed by Lee et al. [11, 12]. Briefly, the approach models spectral Rrs as a function of five independent variables for optically shallow waters, i.e.,

$$R_{rs}(\lambda_1) = F(a_w(\lambda_1), b_{bw}(\lambda_1), \boldsymbol{P,G,X,B,H})$$
$$R_{rs}(\lambda_2) = F(a_w(\lambda_2), b_{bw}(\lambda_2), \boldsymbol{P,G,X,B,H})$$
$$\vdots$$
$$R_{rs}(\lambda_n) = F(a_w(\lambda_n), b_{bw}(\lambda_n), \boldsymbol{P,G,X,B,H}), \quad (8)$$

Here P and G are absorption coefficients of phytoplankton and gelbstoff at 440 nm respectively; X is the backscattering coefficient of suspended particles at 440 nm, B the bottom reflectance at 550 nm, and H the bottom depth. To derive the five unknowns, a spectral optimization scheme with computer processing code (HOPE) has been developed. By varying the values of the five unknowns, the five unknown components are considered derived when the modeled Rrs spectrum best matches the Hyperion spectrum.

5. Results and discussion

The derived water and bottom properties from Hyperion Rrs were compared with those from other independent measurements. Figure 4a presents the derived image of water's total absorption coefficient at 440 nm (a parameter for water turbidity). As expected for a coastal system Fig.4a shows systematic increase of a(440) from offshore to inshore in a pattern parallel to the coastal line. In addition, Fig.4a shows the outflow of in-land waters into the coastal system. As demonstrated, for such a small area (~ 7 km by 20 km) this water optical property is not homogeneous but varies by an order of magnitude. If a method to retrieve bottom properties relies on the assumption of homogeneous water properties, then it will have difficulties for such an area. On the other hand, for pixels that are in parallel to the coast, we see a nearly constant optical property (though progressively increase to coastal line), most likely a result of mixing from tidal flow and alongshore currents.

Fig.4b compares Hyperion a(440) (total absorption coefficient at 440 nm) with in-situ a(440). For the five stations that have a(440) measurements, the stations with lower a(440) values compared very well (average difference is about 10%) between Hyperion results and in-situ measurements. For St.5 and St.6, where a(440) values are about an order of magnitude higher than that of other stations, the average difference in a(440) is about 25%. Because both St.5 and St.6 are very shallow in depth this larger difference may be due to increased bottom reflectance which dominated that from scattering of the water column (see following section). With increased contribution from the bottom there is a much smaller signal contribution from the water column and the accuracy of retrieving water properties is then limited. However, for such complex region, the derived a(440) value is still quite consistent with those from in-situ measurements.

In contrast to the image spatial patterns shown by a(440), the depth image from Hyperion is much different (Fig.5a). Instead of quite uniform pattern in the lower portion of the image shown by a(440), the bathymetry i mage shows distinctive patchiness for that area, with a shallow sandy bar and a deeper channel clearly depicted. Also clearly shown is the deeper ship channel parallel to the coast (known as Hawk channel), and the progressively shallower depth approaching the shore. Compared to the conventional bathymetry chart (see Fig.1a), the bathymetry derived from Hyperion shows excellent consistency with the chart, but Hyperion bathymetry provides better resolution and much more details. Such information is very important for Navy applications and coastal navigation.

Fig.5b compares Hyperion bathymetry with the bottom depth measured at the five stations. For the range of ~2-13 meters, both depths agree with each other very well (less than 10% difference on average). Further, Hyperion bathymetry is compared with the bathymetry derived for the SHOALS system (Fig.5c). For over 70,000 points that have measurements from both systems and covering a range of ~1 – 20 meters, the bathymetry from the two systems show good agreement (average difference is ~15%). Note that the spatial resolution of SHOALS is about 1 meter, while the spatial resolution of Hyperion is about 30 meter, so binning of the lidar data is necessary in order to compare the two. Also, Hyperion has an uncertainty of ~100 m in ground registration. With these sources of errors in mind, an overall error of ~15% in bathymetry from Hyperion is quite promising, suggesting significant potentials of using Hyperion for observation of coastal regions in both water colum and bottom properties.

6. Conclusions

We have demonstrated that with our innovative approach of deriving Rrs from Hyperion, excellent Rrs spectrum could be obtained from Hyperion data. This method avoids the rigid requirement of accurate radiometric calibration of the sensor, and overcome commonly encountered problem of negative Rrs in the blue when using standard atmosphere correction algorithm.

Feed Hyperion Rrs to an advanced algorithm to derive properties of water column and bottom, we also retrieved surprisingly impressive results for a sensor that was not designed for water studies. This has tremendous implications for other future sensors and existing sensors. The implication is that such techniques can extend the utility of sensors primarily designed for land applications for some coastal applications. While these results are not meant to suggest land satellites can be automatically be used for water studies. It does suggest that information can be obtained from such sensors that can benefit coastal applications for the military and commercial applications.

Acknowledgements

Financial support for this study was provided by NASA. Georeference of the Hyperion image by Judie Dye is greatly appreciated.

Reference:

1. Z. P. Lee and K. L. Carder, "Effect of spectral band numbers on the retrieval of water column and bottom properties from ocean color data," Applied Optics **41**, 2191-2201 (2002).
2. S. G. Ungar, "Overview of the Earth Observing One (EO-1) Mission," IEEE (2002).
3. V. E. Brando and A. G. Dekker, "Satellite hyperspectral remote sensing for estimating estuarine and coastal water quality," IEEE TRANSACTIONS ON GEOSCIENCE AND REMOTE SENSING 41(6), 1378-1387 (2003).
4. R. K. Clark, T. H. Fay, and C. L. Walker, "Bathymetry calculations with Landsat 4 TM imagery under a generalized ratio assumption," Applied Optics **26**, 4036-4038 (1987).
5. D. R. Lyzenga, "Shallow-water bathymetry using combined lidar and passive multispectral scanner data," Int. J. Remote Sensing **6**, 115-125 (1985).
6. H. R. Gordon, "Removal of atmospheric effects from satellite imagery of the oceans," Applied Optics **17**, 1631-1636 (1978).
7. H. R. Gordon and M. Wang, "Retrieval of water-leaving radiance and aerosol optical thickness over oceans with SeaWiFS: A

preliminary algorithm," Applied Optics **33**, 443-452 (1994).

8. P. Barry, P. Jarecke, and J. Pearlman, "Radiometric calibration validation of the Hyperion instrument using ground truth at a site in Lake Frome, Australia," SPIE (2001).
9. P. Reinersman, K. L. Carder, and F. R. Chen, "Satellite-sensor calibration verification with the cloud-shadow method," Applied Optics **37**(24), 5541-5549 (1998).
10. W. W. Gregg and K. L. Carder, "A simple spectral solar irradiance model for cloudless maritime atmospheres," Limnol. Oceanogr. **35**, 1657-1675 (1990).
11. Z. P. Lee, K. L. Carder, C. D. Mobley, R. G. Steward, and J. S. Patch, "Hyperspectral remote sensing for shallow waters: 2. Deriving bottom depths and water properties by optimization," Applied Optics **38**, 3831-3843 (1999).
12. Z. P. Lee, K. L. Carder, R. F. Chen, and T. G. Peacock, "Properties of the water column and bottom derived from AVIRIS data," J. Geophy. Res **106**, 11639-11652 (2001).

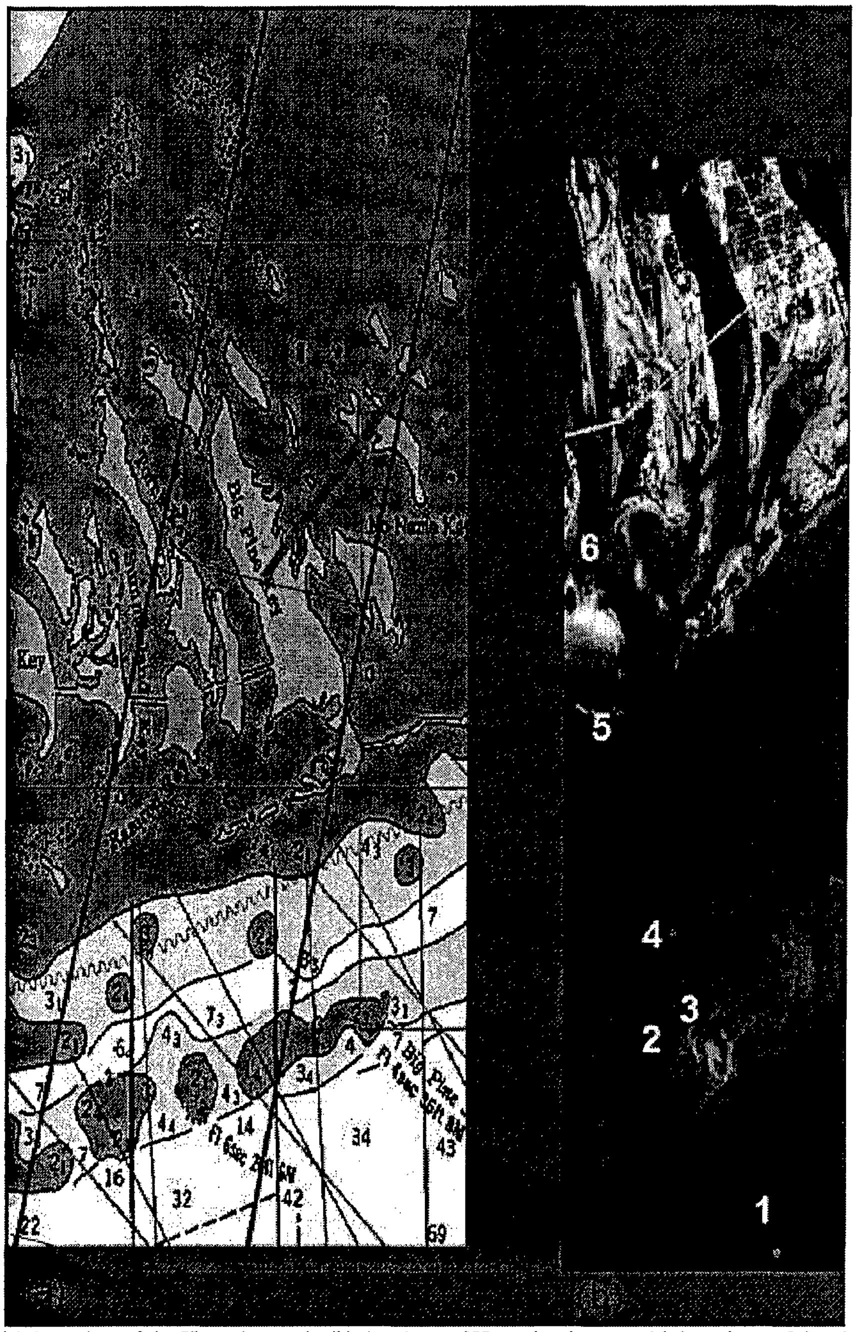

Figure 1. (a) Location of the Hyperion path. (b) A subset of Hyperion image with locations of the six stations with in-situ measurements.

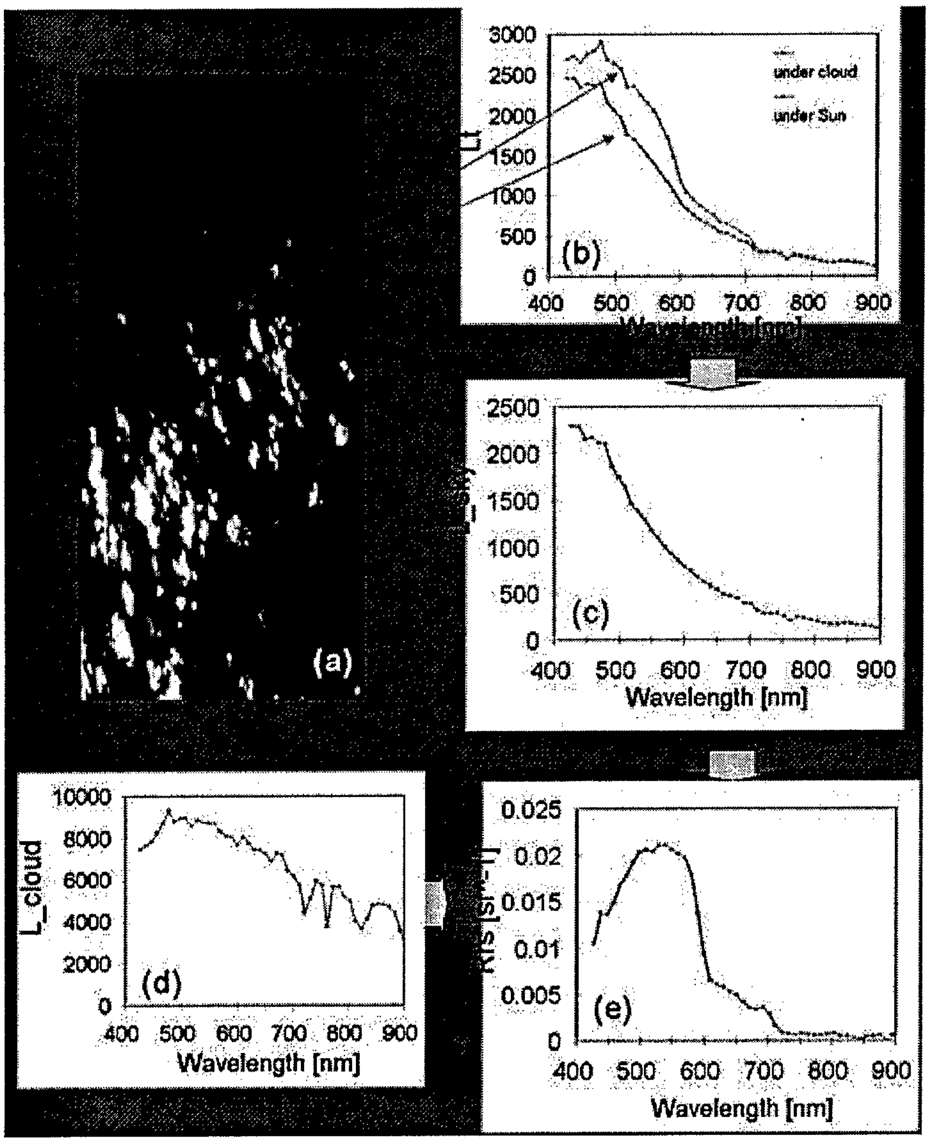

Figure 2. Demonstration of " Cloud-Shadow Technique. Panel (a) shows selection of a pair of pixels under the Sun and under cloud; (b) L_t of the two pixels; (c) derived L_sky from this pair; (d) L_t from top of the clouds; and (e) calculated Rrs for the pixel under the Sun (Fig.2a).

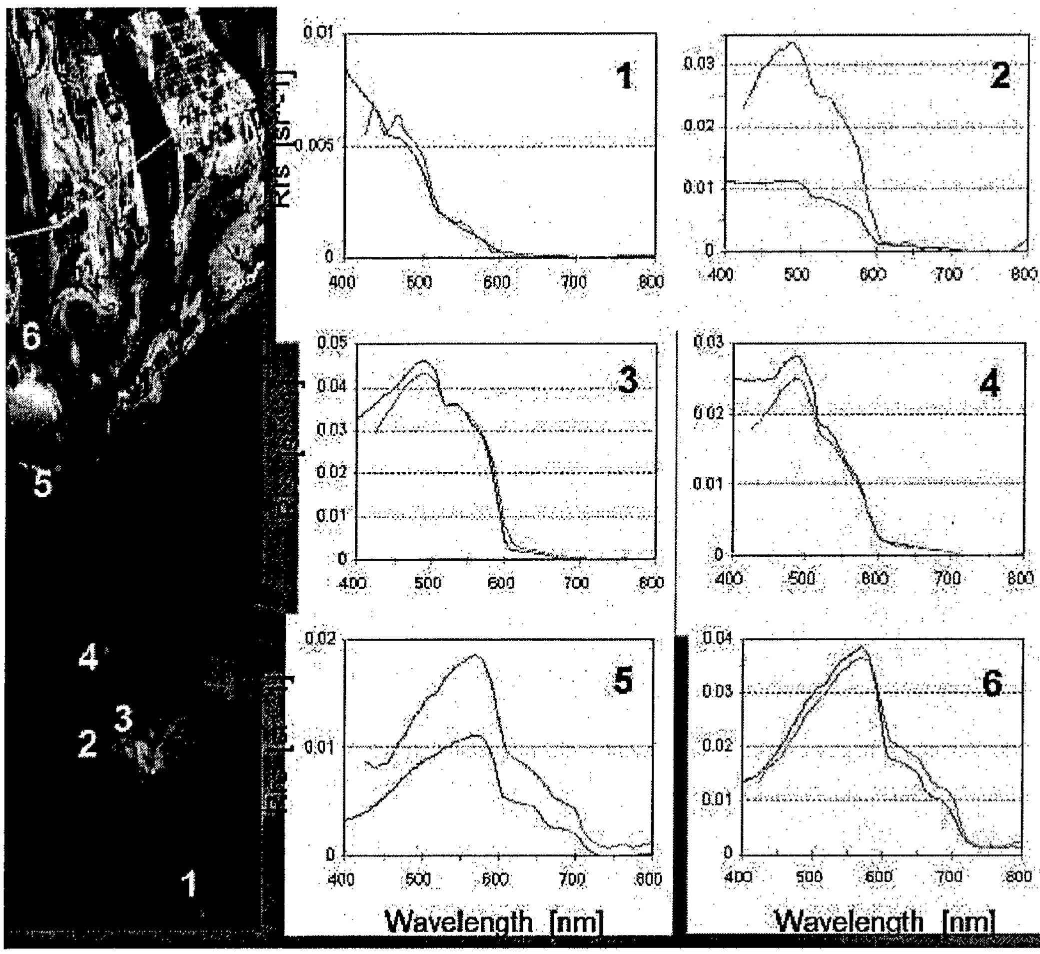

Figure 3. Rrs from Hyperion (green line) compared with Rrs from field measurements (red line) for the six stations.

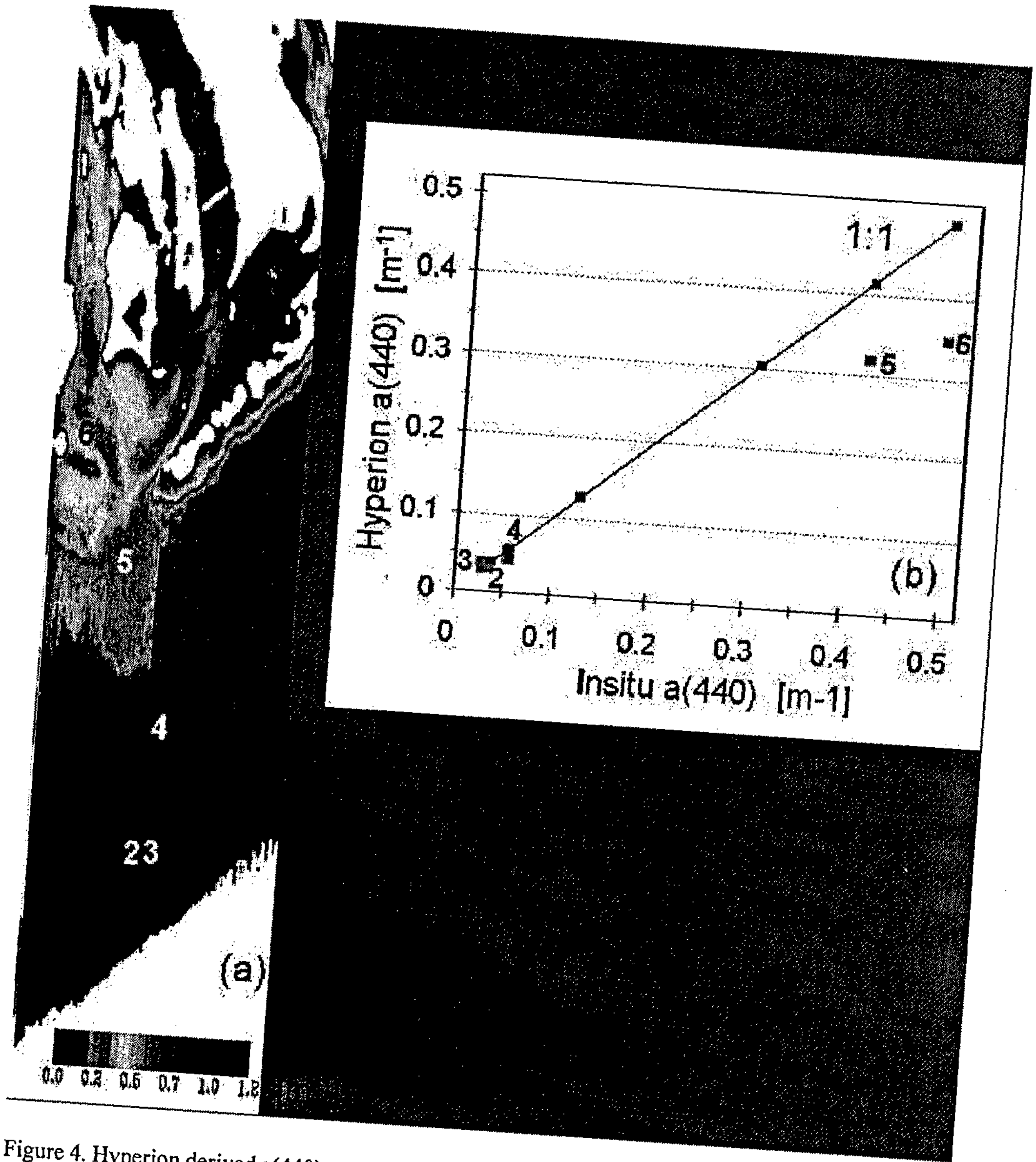

Figure 4. Hyperion derived a(440) compared with a(440) from field measurements.

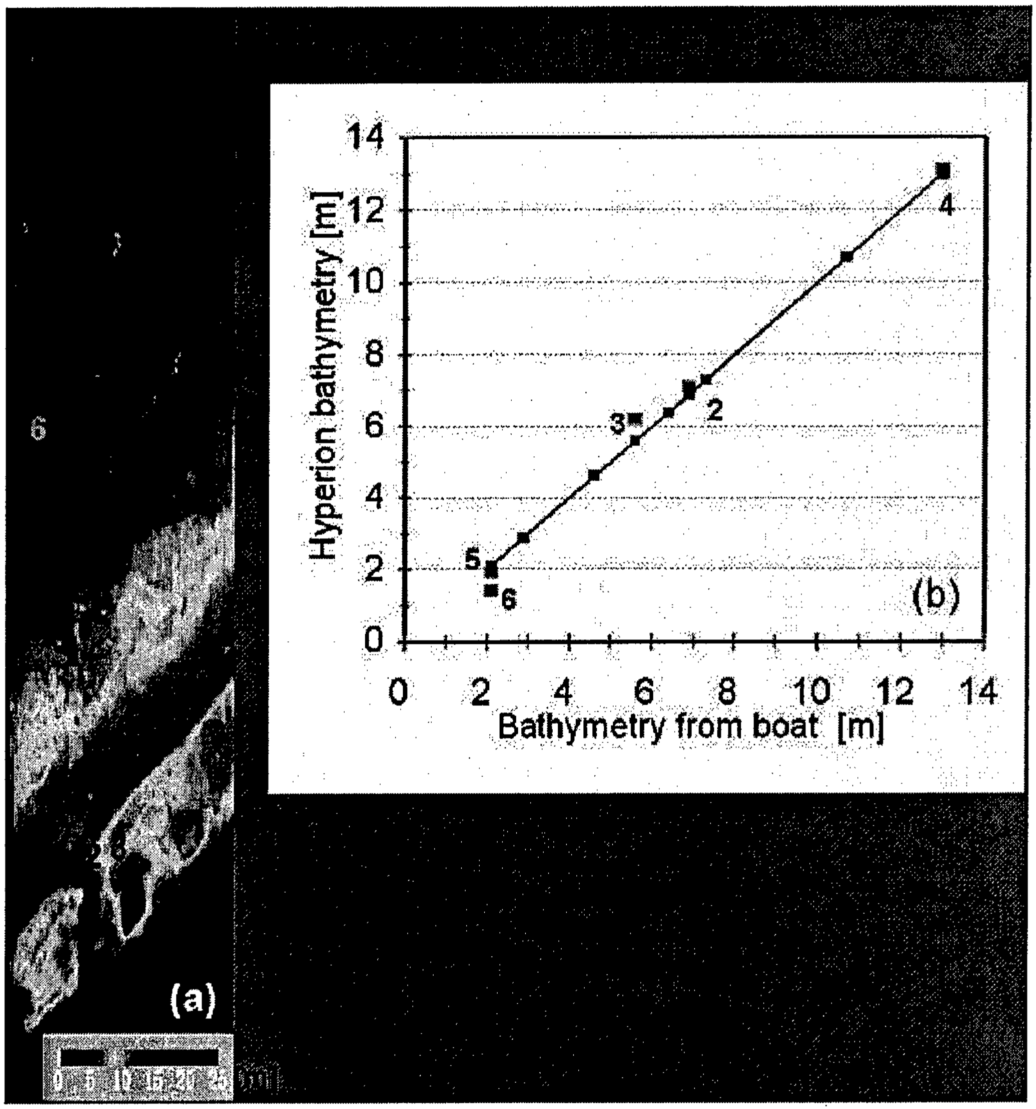

Figure 5. (a) Bathymetry image derived from Hyperion; (b) bathymetry compared to in-situ value collected from shipboard measurements.

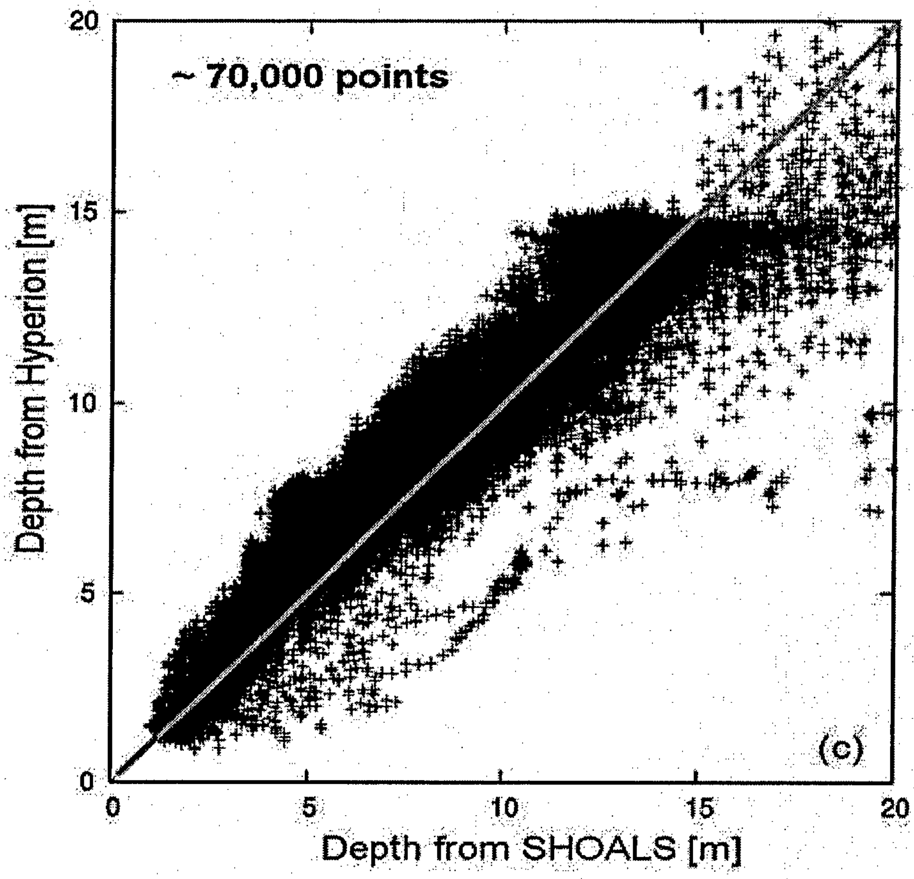

Figure 5c. Comparison of Hyperion bathymetry and SHOALS lidar-measured bathymetry.

REPORT DOCUMENTATION PAGE	Form Approved OMB No. 0704-0188

1. REPORT DATE *(DD-MM-YYYY)*	2. REPORT TYPE	3. DATES COVERED *(From - To)*
9-6-2006	Conference Proceedings (not refereed)	

4. TITLE AND SUBTITLE
Bathymetry of Shallow Coastal Regions Derived from Space-borne Hyperspectral Sensor

5a. CONTRACT NUMBER

5b. GRANT NUMBER

5c. PROGRAM ELEMENT NUMBER
PE0601153N

6. AUTHOR(S)
Z. Lee, B.J. Casey, A.R. Parsons, W.A. Goode, A.D. Weidemann, R.A. Arnone

5d. PROJECT NUMBER

5e. TASK NUMBER

5f. WORK UNIT NUMBER
73-8028-B5

7. PERFORMING ORGANIZATION NAME(S) AND ADDRESS(ES)
Naval Research Laboratory
Oceanography Division
Stennis Space Center, MS 39529-5004

8. PERFORMING ORGANIZATION REPORT NUMBER
NRL/PP/7330-05-5053

9. SPONSORING/MONITORING AGENCY NAME(S) AND ADDRESS(ES)
Office of Naval Research
800 N. Quincy St.
Arlington, VA 22217-5660

10. SPONSOR/MONITOR'S ACRONYM(S)
ONR

11. SPONSOR/MONITOR'S REPORT NUMBER(S)

12. DISTRIBUTION/AVAILABILITY STATEMENT
Approved for public release, distribution is unlimited.

13. SUPPLEMENTARY NOTES

14. ABSTRACT
Hyperion is a hyperspectral sensor on board NASA's EO-1 satellite. Its spatial resolution is about 30 m with a swath of ~7 Km. Though Hyperion was not designed for ocean studies, its unique spectral configuration (430 nm-2400 nm with a ~10 nm step) makes it especially attractive to study the effectiveness of such kind of sensor for observing complex coastal waters. In this study, Hyperion data over two sites of the Florida coasts were acquired, with one focused on the clear Key West waters, and the other focused on the relatively turbid Tampa Bay waters. From both data sets, water properties and bottom bathymetry were simultaneously derived from atmosphere corrected Hyperion data using a spectral matching technique. More importantly, in the top-to-bottom processing of Hyperion data, there was no use of *a prior* or ground truth information. For the Key West site, derived bathymetry and water properties were validated with NAVOCEANO CHARTS (active bathymetric LIDAR system) and field measurements, respectively. It is found that the retrieved depths (in a range of ~1-20 m) match LIDAR depths very well (~15% average error), indicating significant potential of using hyperspectral satellite sensor for efficient and repetitive observation of shallow coastal regions.

15. SUBJECT TERMS
Hyperion; bathymetry; hyperspectral satellite sensors

16. SECURITY CLASSIFICATION OF: a. REPORT	b. ABSTRACT	c. THIS PAGE	17. LIMITATION OF ABSTRACT	18. NUMBER OF PAGES	19a. NAME OF RESPONSIBLE PERSON
Unclassified	Unclassified	Unclassified	UL	11	Zhongping Lee
					19b. TELEPHONE NUMBER *(Include area code)* (228) 688-4873

PUBLICATION OR PRESENTATION RELEASE REQUEST

Pubkey: 4606 NRLINST 5600.2

1. REFERENCES AND ENCLOSURES	2. TYPE OF PUBLICATION OR PRESENTATION	3. ADMINISTRATIVE INFORMATION
Ref: (a) NRL Instruction 5600.2 (b) NRL Instruction 5510.40D Encl: (1) Two copies of subject paper (or abstract)	( ) Abstract only, published ( ) Book ( ) Conference Proceedings (refereed) ( ) Invited speaker ( ) Journal article (refereed) ( ) Oral Presentation, published ( ) Other, explain ( ) Abstract only, not published ( ) Book chapter (X) Conference Proceedings (not refereed) ( ) Multimedia report ( ) Journal article (not refereed) ( ) Oral Presentation, not published	STRN NRL/PP/7330-05-5303 Route Sheet No. 7330/ Job Order No. 73-8028-B5-5 Classification X U ___ C Sponsor ONR BASE approval obtained ___ yes X no

4. AUTHOR

Title of Paper or Presentation

Bathymetry of Shallow Coastal Regions Derived from Space-borne Hyperspectral Sensor

Author(s) Name(s) *(First,MI,Last), Code, Affiliation if not NRL*

Zhongping Lee, Brandon J Casey, Arthur R. Parsons, Wesley A. Goode, Alan D. Weidemann, Robert A Arnone

It is intended to offer this paper to the **Oceans 2005 MTS/IEEE Conference** *(Name of Conference)*

19-SEP - 23-SEP-2005, Washington, DC, Unclassified
(Date, Place and Classification of Conference)

and/or for publication in **Oceans 2005 MTS/IEEE Conference, Unclassified** *(Name and Classification of Publication)* ___ *(Name of Publisher)*

After presentation or publication, pertinent publication/presentation data will be entered in the publications data base, in accordance with reference (a).
It is the opinion of the author that the subject paper (is ___) (is not X) classified, in accordance with reference (b).
This paper does not violate any disclosure of trade secrets or suggestions of outside individuals or concerns which have been communicated to the Laboratory in confidence. This paper (does ___) (does not X) contain any militarily critical technology.
This subject paper (has ___) (has never X) been incorporated in an official NRL Report.

Zhongping Lee, 7333 — for R Arnone
Name and Code *(Principal Author)* (Signature)

5. ROUTING/APPROVAL

CODE	SIGNATURE	DATE	COMMENTS
Author(s) Lee	R Arnone	8/4	NEEDED BY 29 Aug 05
Section Head Gould	Bob Gould	8/4	
Branch Head **Robert A Arnone, 7330**	R Arnone	8/4	
Division Head **Ruth H. Preller, 7300**	Ruth H Preller	8/5	1. Release of this paper is approved. 2. To the best knowledge of this Division, the subject matter of this paper (has ___) (has never X) been classified.
Security, Code **7030.1**	[illegible]	8/22/05	1. Paper or abstract was released. 2. A ~~copy is filed in this office~~ @ SSC-336-05
Office of Counsel, Code **1008.3**	[illegible]	8/12/05	
ADOR/Director NCST **E.O. Hartwig, 7000**			
Public Affairs *(Unclassified/ Unlimited Only)*, Code **7030.4**	Becky Rotundo	8/11/05	
Division, Code			
Author, Code			

HQ-NRL 5511/6 (Rev. 12-98) (e) THIS FORM CANCELS AND SUPERSEDES ALL PREVIOUS VERSIONS